

In-field visualisation of water infiltration and soluble salt transport

Andrei Rozanov^A and Willem de Clercq^A

^ADepartment of Soil Science, University of Stellenbosch, 7600 South Africa, Email dar@sun.ac.za

Abstract

Visualisation of saline water infiltration pattern was done with digital photography. KI was added to water applied through double-ring infiltrometer. Fine layers of soil were excavated on completion of infiltration test and spray-treated with starch and pyroxide to develop blue colour shades from reaction with Iodine. Images of both vertical and sequential horizontal sections of the wetted profile were acquired. The images were rectified and post-processed to isolate and qualify the frontal and preferential flow.

Key Words

Preferential flow, flow visualisation, soil salinity.

Introduction

The study of salt transport in the lower catchment of the Berg River (Western Cape, South Africa) has raised questions whether it may be considerably affected by macropore water flow at the scale of soil profile. Field observations of cracks on the clayey soil surface in some parts of the catchment and multiple instances of termite activity suggested that preferential water flow may be present in the system. A quick test showed that flooding with small quantities of water may have substantial effect on the pattern of instant water infiltration in a cracking soil (Figure 1). The excavation of the flooded soil to the depth of some 5 cm demonstrated that only small fraction of the total soil volume around the cracks was wetted leaving most of the large blocky aggregates in dry state (Figure 1 c). This observation inspired detailed studies of infiltration patterns using a colour tracer to identify preferential flow pathways. Various in-situ (Gazis *et al.* 2004; Forrer *et al.* 2000) and ex-situ (Mooney 2006) methods of visualising the process were considered and slightly modified method based on iodine-starch staining (Hangena *et al.* 2003) was selected.



a) cracks on soil surface

b) flooding of cracked soil

c) excavation of flooded soil

Figure 1. Observations of instant preferential flow through cracked topsoil.

Methods

Field experiments

Soils of Glenrosa form (*Lithic Cambisol*) on Malmesbury shales were selected for the experiment, being some of the dominant soils according to the results of the soil survey. Standard double ring infiltrometer was used and pressure potential of 100 mm was maintained throughout the experiment. On completion of infiltration the water was allowed to drain for a short period of time (up to 2 hours) and both vertical and horizontal sections of the soil were exposed. One vertical and several horizontal sections were made per soil profile.

Summer infiltration

Three double ring infiltration sites were established as following.

- Soil with few or no visible cracks on the surface next to one of the soil survey profiles.
- Soil with visible termite activity.
- Soil with visible sediment accumulation and extensive cracking above the contour bank.

The experiments included:

- determination of infiltration rates

- b) determination of soil bulk density and moisture content
- c) visualization of water flow with KI-starch reaction.

Considering high variability of climate, it was decided to conduct the experiments twice – in summer and winter to compare infiltration rates for desiccated and pre-wetted soil.

Winter infiltration in wheat fields

Two sites were selected to repeat infiltration measurements with double ring infiltrometer for comparison with summer results. In addition two runs of rainfall simulation were conducted for observation on larger area in conditions of free run-off instead of a pressurized double ring infiltrometer system.

Visualisation

KI (potassium iodide) was selected as a tracer for several reasons.

- a) reliable reaction with starch allowing high visibility in the soil.
- b) high solubility and behaviour in soil, which would be similar to that of modelled salt fluxes and distributions.

Concentration of KI in water was 7% (half the amount used by Hangena *et al.* 2003), which was deemed to be sufficient considering the light background colour of the soil.

Soil sections were sprayed with (5%) pyroxide solution to facilitate release of I_2 from KI and further sprayed with household starch spray from a pressurized canister. The reaction of iodine with starch was considered completed after 10 mins and digital photographs in RAW format were taken with Canon G5 camera for image processing. The images were corner-stone projected and converted into the LAB colour space.

Results and discussion

The images were converted into the LAB colour space for enhancement (Figure 2). The processing of enhanced images is still under way and the exact methodology is in the development stage.



Figure 2. Image enhancement by contrasting the the b layer in LAB colour space.

The current problems in image processing that have to be solved are

- a) variations in illumination within the photograph.
- b) influence of I_2 and starch concentrations on the colour characteristics.
- c) the influence of background colour variations on colour characteristics of the stained area.

The observed infiltration rates were extremely slow, though large unrecorded volumes of water were required to fill up the infiltrometers. Over 24 hours of infiltration resulted in very shallow water penetration as wetting front progressed (Figure 3a), however deep water channeling was observed in some macropores of the lithocutanic B horizon (Figure 3b). One of the important points was that the observed pattern of iodine distribution in the soil was not corresponding well with the measured bulked values of soil moisture content noted by Weiler and Flühler (2003) for various dyes. Increase in moisture content was observed deeper than the visible penetration of the wetting front. The most reasonable explanation for that is the attenuation of KI for clay and participation in exchange reactions in soil. The soil was performing as a chromatographic column leaving most of the KI at the top of the profile. This was somewhat aggravated by relatively low concentrations of KI, and possibly some patchiness in distribution of pyroxide and starch over the sprayed surface, though every effort was made to ensure a dense mist spraying.



a) Frontal infiltration observed in the lithocutanic (cambic) B horizon



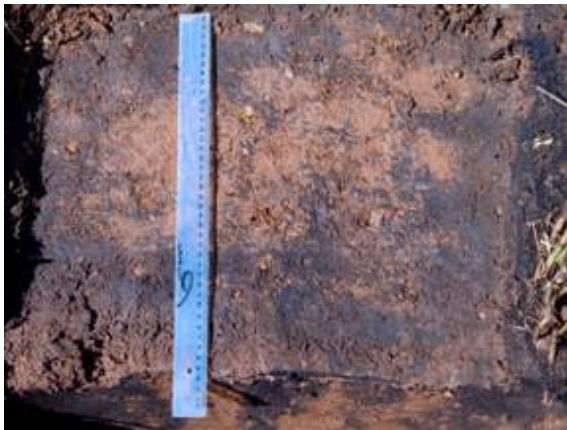
b) spot of iodine-starch complex channelled to the depth of 53 cm

Figure 3. Infiltration into the lithocutanic B horizon of the Glonrosa soil at Goudertrou.

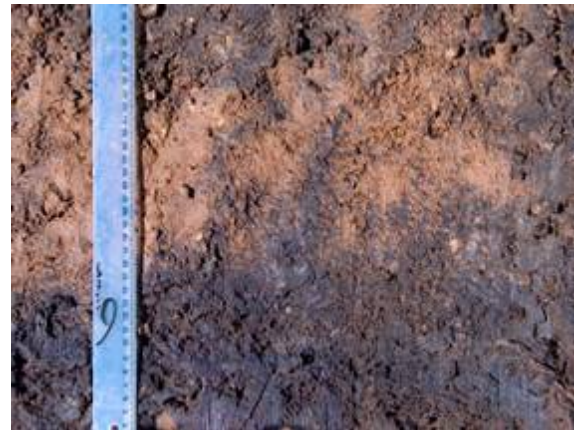
During the winter run of the infiltration experiments the infiltration rates were higher, seemingly due to higher initial moisture content of the soil and recent land preparation. It was also observed that presence of plants in the field improves infiltration by channelling water along the stalk towards the rooting zone and, ultimately into the prepared row of wheat. This phenomenon was observed both in the ring infiltrometer and under rainfall simulator (Figures 4 and 5).

In case of rainfall simulation sub-samples of wheat were taken from irrigated and non-irrigated parts of the field, showing water interception by wheat averaging at 85% of total dry mass. Interception by the canopy of the crop leads to shading of the soil and channelling of water. However, since the same phenomenon was observed in the flooded double ring infiltrometer experiment, one can say that two mechanisms are at play here:

- a) interception by the canopy and channelling of rain water along the stalks of wheat;
- b) channelling of water through the soil along the root canals.



a) rainfall simulator



b) ring infiltrometer

Figure 4. Effect of furrows with wheat on water infiltration at the depth of 6 cm.

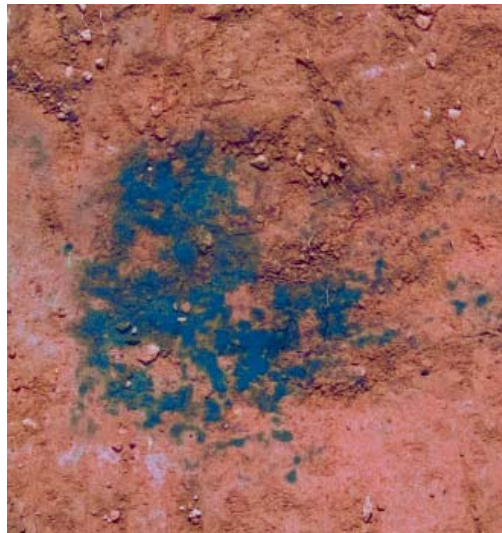
Image enhancement considerably improves the identification of wetted pores through the oriole effected formed on the boundary of the pore and adjacent surface treated with pyroxide and starch (Figure 5). It allows to semi-automate the process of image classification and provides sharp boundaries.

Conclusion

It was shown that KI may be successfully used as a tracer for visualizing water infiltration and soluble salt movement against the contrasting background of light-coloured soil. The method is also inexpensive, but requires further calibration and image interpretation studies. Quantification of water infiltration using the suggested visualisation technique is problematic due to partial dye retention and may be further complicated by iodine volatilisation and transport through air-filled pores. The errors introduced by the above effects require further study and quantification. The main advantage of this method is the possibility of in-field visualisation as opposed to core sample analysis, and imposes practically no restrictions either the size of the



a) raw image



b) enhanced image showing distinct boundary oriole effect around the wetted zone

Figure 5. Effect of wheat roots on water infiltration at the depth of 30 cm.

studied macropores or that of the experimental plot itself if KI solution is applied through rainfall simulator or irrigation system. The method allowed to distinguish between the effect of land preparation practices and biological macropores on preferential flow patterns in the bulk volume of soil under wheat fields and may be applied as a useful tool in the study of cultivation systems and implements.

References

- Ferrer J, Papritz I, Kasteel A, Flühler R, Luca HD (2000) Quantifying dye tracers in soil profiles by image processing. *European Journal of Soil Science* **51**, 313–322
- Gazis C, Feng X (2004) A stable isotope study of soil water: evidence for mixing and preferential flow paths. *Geoderma* **119**, 97– 111
- Hangena E, Gerke HH, Schaaf W, Hüttl RF (2003) Flow path visualization in a lignitic mine soil using iodine–starch staining. *Geoderma* **120**,121–135
- Mooney SJ (2006) Three-dimensional visualization and quantification of soil macroporosity and water flow patterns using computed tomography. *Soil Use and Management* **18**, 142-151.
- Weiler M, Flühler H (2003) Inferring flow types from dye patterns in macroporous soils. *Geoderma* **120**,137–153